3D CFD Modelling of the Airflow and Heat Transfer in Cold Room Filled with Dates

Zina Ghiloufi, Tahar Khir

Abstract—A transient three-dimensional computational fluid dynamics (CFD) model is developed to determine the velocity and temperature distribution in different positions cold room during pre-cooling of dates. The turbulence model used is the k-ω Shear Stress Transport (SST) with the standard wall function, the air. The numerical results obtained show that cooling rate is not uniform inside the room; the product at the medium of room has a slower cooling rate. This cooling heterogeneity has a large effect on the energy consumption during cold storage.

Keywords—Numerical simulation, CFD, k-ω (SST), cold room, dates, cooling rate.

I. INTRODUCTION

IN the South of Tunisia the storage of dates constitutes an important economic activity for the local market as well as for export. However, the installations of cold rooms are generally performed without respect to the standard design conditions; these expose the products to deterioration risks and affect their nutritive quality. In the purpose to define suitable storage conditions for dates and avoid the losses, a numerical study is conducted in our research unit on air flow and temperature distribution inside the cold store room equipped with package bins arranged in rows. The main object of this study is to analyze the thermal behavior of pre-cooling.

Several researches are performed on the complexity of airflow and the heat transfer product-air in cold store rooms. Models are developed to predict the cooling conditions using CFD. Nahor et al. established 3D model airflow and heat transfer with CFD in cold store room used to preserve pears [1]. The model k-ε is used to study the airflow profile and given results close to experimental value. Son et al. compared two models: 2D and 3D CFD, and suggest that the 2D model can determine the cooling behavior of products in cold store room correctly [2]. The popular approach used in cooling model is the porous medium. Hoang et al. used two approaches to simulate the cooling kinetic of four apple pallets in a cold store room with CFD [3]. For the first approach, pallets are considered as porous medium. While for the second approach, they considered each apple pallets as eighth solid blocks. The results of both approaches show a good agreement with experimental results taken from the literature. All research works demonstrate that temperature product diminution was faster in few initial hours of cooling and then become slower with exponential diminution behavior [4]. Many factors affect the cooling rate in the room: Temperature storage, thermal

properties of product, airflow distribution, and package design [5].

For this paper a numerical study using CFD is established on the airflow and temperature distribution in a cold store room used to preserve about ten tons of dates.

II. NUMERICAL MODELS

A. Computational Domain

Using the guidelines of [6], the cold room sizes are determined. The overall sizes of cold room are L x W x H: 5.6 m x3.62 m x 3.3 m, filled with 10 tons of date distributed in 432 bins (Fig. 1). The air flow of cooling unit is about12300 m^3h^{-1} provided by three fans of 0.45 m of diameter and rotating at 1500 RPM as shown in Fig. 1. Taking into consideration the small sizes of dates, each bin is considered as solid block of $64 \times 62 \times 11$ cm of sizes. Since the bins are partially filled with dates. These bins are distributed in three rows in the cold room and spaced from one another 0.7 m.
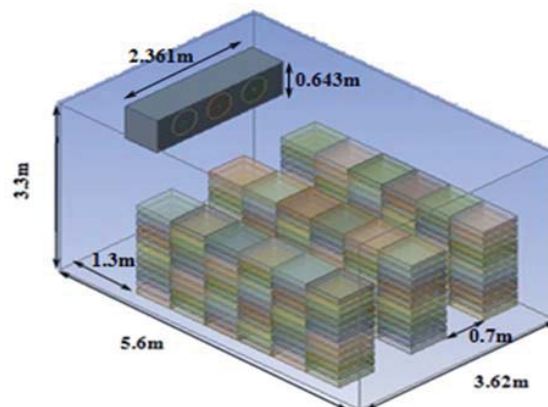

Fig. 1 Design of cold room and bins arrangement

The cooling rate is accomplished through two convective heat transfer modes: air-product and air-package. Also the conduction heat transfer inside the block of date is considered.

For heat transfer simulation, steady state is considered with initial product temperature of 309 K. whereas the air flow temperature is equal to 276 K. The heat transfer coefficient between date and air, h $_{date-air}$, is given by:

$$h_{dates-air} = \frac{Q}{T_p - T_{air}} \qquad (1)$$

Zina Ghiloufi is with the National Engineering School, Tunisia (e-mail: ghiloufizina17@hotmail.com).

where, Q: normal heat flux at interface air – dates; T_p: Temperature of date (°K); T_{air}: Temperature of air (°K).

The natural convection is neglected regarding forced one. Also the heat respiration did not have a significant effect on cooling fresh horticultural aliments [7].

The air and date properties [8] are considered as constant and presented on Table I.

TABLE I
PROPRIETIES OF AIR AND DATES

μ_a	1.72e-5 kg.m^{-1}.s^{-1}
ρ_a	1.293 kg.m^{-3}
c_{pa}	1004 Jkg^{-1}K^{-1}
λ_a	24.07e-3 Wm^{-1}K^{-1}
ρ_{dattes}	1320 kgm^{-3}
$c_{pdattes}$	2310 Jkg^{-3}K^{-1}
λ_{dattes}	0.337 Wm^{-1}K^{-1}

μ, λ, ρ and c_p are the dynamic viscosity, the thermal conductivity, the density and the heat capacity at constant pressure respectively. a: refer to air.

B. Governing Equations

The equations of Reynolds-Averaged Navier Stokes (RANS) in three-dimensional is used to determine the air velocity and heat transfer fields. The turbulence model k-ω SST is used. This model presents a good performance to describe the turbulent and studying the heat transfer at the interface air-product regime of cold store room [3]. The governing equations can be expressed as follows:

Continuity equation

$$\frac{\partial \overline{u_i}}{\partial x_i} = 0 \qquad (2)$$

Momentum equation:

$$\rho_f \frac{\partial \overline{u_i} \overline{u_j}}{\partial x_j} = -\frac{\partial \overline{p}}{\partial x_i} + \frac{\partial}{\partial x_j}[\mu(\frac{\partial \overline{u_i}}{\partial x_j} + \frac{\partial \overline{u_j}}{\partial x_i})] - \rho_f \frac{\partial \overline{u_i' u_j'}}{\partial x_j} \qquad (3)$$

The Reynolds stress term given in (3) is calculated according to Boussinesq hypothesis as:

$$\rho_f \overline{u_i' u_j'} = \mu_t (\frac{\partial \overline{u_i}}{\partial x_j} + \frac{\partial \overline{u_j}}{\partial x_i}) - \frac{2}{3} \rho_f k \delta_{ij} \qquad (4)$$

Energy equation

$$\frac{\partial \overline{T_f}}{\partial t} + \overline{u_i} \frac{\partial \overline{T_f}}{\partial x_i} + \frac{1}{\rho_f c_{pf}} \frac{\partial \overline{p}}{\partial x_i}) = \frac{\partial}{\partial x_i}(\frac{\lambda_{eff}}{\rho_f c_{pf}} \frac{\partial \overline{T_f}}{\partial x_i}) \qquad (5)$$

where, f: fluid; eff: effective; u: fluid velocity (m.s^{-1}); T: temperature (K); P: pressure (Pa); k: turbulence kinetic energy (m^{2}K); t: time (s).

C. Meshing

The section of room is divided in 16818637 cells and 5182978 nodes. The generated meshing is considered using ANSYS Mesher code.

D. Boundary Conditions

1. Airflow

One of the constraints in the air distribution study of cold room is the modeling of the fan blades movement; in our work we used this function to decrier the air velocity inlet of chamber.

Axial velocity

$$u_{axial} = \frac{v_{max} r}{R_{max}}. \qquad (6)$$

Tangential velocity

$$u_{tan\,gential} = C_s r\omega \qquad (7)$$

where, r: radius of the calculated point (m); R: fan radius (m); C_s: swirling coefficients; ω: angular fan speed (rad.s^{-1}); u_{max}: maximal velocity (m.s^{-1}).

2. Wall

The wall and the solid blocks are modeled as no-slip walls with zero roughness. In transient state simulation, the solid bocks give the convective heat transfer coefficient calculated in steady state.

3. Outlet

Outflow boundary condition is applied at the air returning section assuming zero normal gradients for all flow variables except pressure.

E. Numerical Simulation

The fluent 16.1 is used to perform the numerical simulation. The diffusion-convection term is discretized with simple scheme. The overall accuracy of the discretisation was in second-order. The model is solved for the velocity field in steady state with mass residuals less than 10-3. Then the model was solved for energy equation in transient regime.

III. RESULTS

A. Airflow

The cold air blown by the fan flow to the end of cold room where it hits the vertical wall parallel to the evaporator and coming back with high velocity (1.7 m.s^{-1}) is close to the floor (Fig. 2); at the return zone, a part of air is entrained by the supply air jet (Fig. 2) and the second part returns the evaporator. The low velocity magnitude is located at the cold room medium; this air distribution will have great effect on the cooling kinetic of stored product.
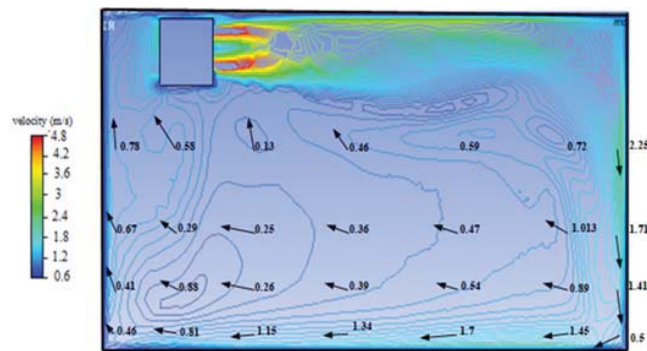
Fig. 2 Air flow

B. Temperature Distribution

After 4 hours of cooling, the temperature distribution of three positions inside the cold room is shown in Fig. 1.

In the three plans, the bins still hotter than the surrounding air. The cold air (276 K) is located near the right wall; in this side the product temperature attains 296 K. The warmer air (284 K) is located in the return zone (near the cooling unit) after the heat exchange with the hot product. The difference in the cooling rate of product is more clear at the medium of the cold room where the product temperature in this position is still high than 296 K, and the air temperature was relatively high (285 K) near the bins.

Plan at the left side of room

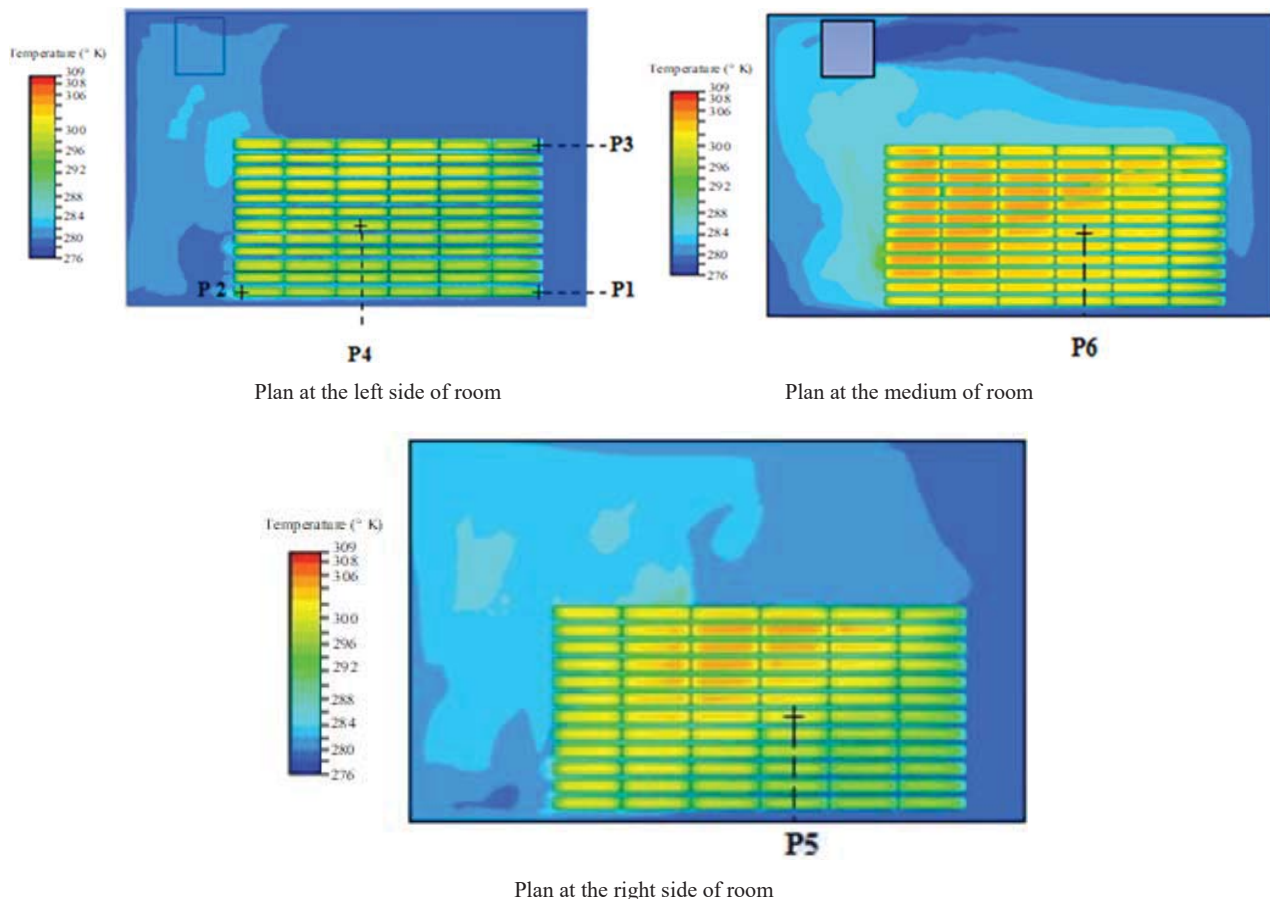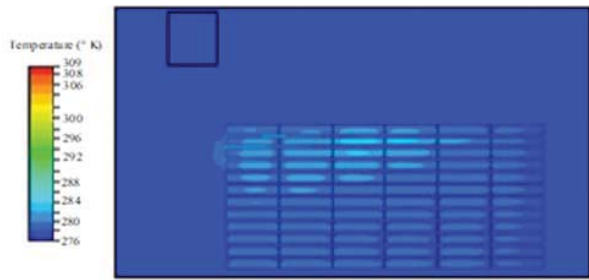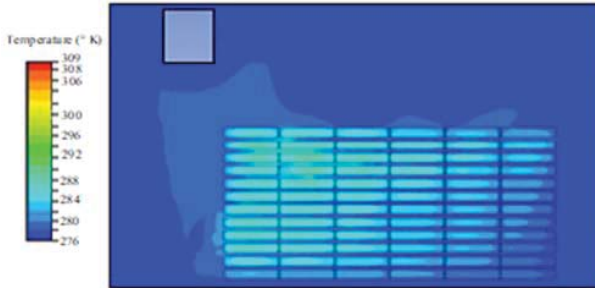Plan at the medium of room

Plan at the right side of room

Fig. 3 Temperature distribution after 4 hours of cooling in three positions inside the cold room

After 25 hours cooling, the temperature distribution of the cold room becomes more homogenous as shown in Fig. 4.

Plan at the left side of room

Plan at the medium of room

Plan at the right side of room

Fig. 4 Distribution of temperature after 25 hours of cooling for three positions in room

The product at the left side becomes colder than the product in other positions in the room. The slower cooling locate in the room medium; where the product temperature still higher than the 285 K.

To more present the cooling heterogeneous inside the room, a dimensionless number Y is defined to characterize the cooling kinetic of product.

$$Y = \frac{(T - T_f)}{(T_i - T_f)}$$

where T_i: initial product temperature; T_f: storage temperature.

Two important value of Y, The Half Cooling Time (Y=0.5) and the Seven-Eighths Cooling Time SECT (Y= 0.125), can depict the cooling rate behavior [4].

Table II shows the HCT of product in various positions, the slow HCT locate in position one P1 (Fig 1) equal to 4.2 hours. The high HCT detect in the medium of cold room P6 (Fig. 1) where it attains the HCT after 11 hours.

The HCT shows that cooling time is heterogeneous in different positions inside the cold room.

TABLE II
THE HCT AT SEVERAL PRODUCT POSITIONS

position	HCT (h)
P1	4,2
P2	6
P3	4,8
P4	7
P5	8
P6	11

Fig. 5 shows the average cooling rate $Y_{average}$ at the medium product bins of three rows. Fig. 5 shows that the cooling rate average at the medium of three rows is not uniform, where the two rows (at the left and right side of room) have the same cooling rate during the refrigerate period. The product at these positions reach the half cooling time HCT (Y=0.5) after about 12 cooling hours. However, the medium row attains the HCT after 14 hours.

This heterogeneity increases in the second part of cooling period where the product in the left and right row attains SECT after 25 hours; the storage temperature (276 K) reaches after 35 hours, whereas the medium row temperature still higher than the desired temperature. This cooling time lag between the three rows increases the energy consumption and consequently the cooling cost. Fig. 6 presents that the row in the medium needs about more power (260 kW) than at the two other rows (160 kW).
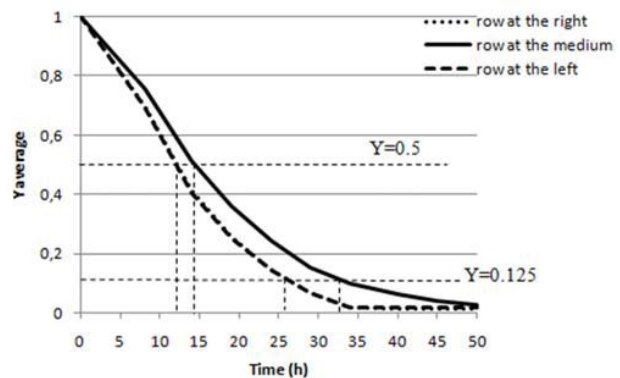

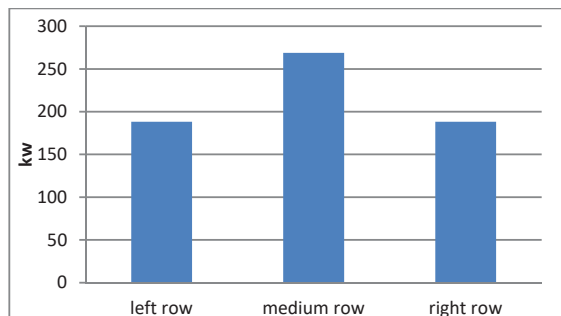Fig. 5 Cooling rate average variation at the medium of three rows

Fig. 6 Energy consumption of three rows

IV. Conclusion

Numerical simulation is conducted to predict the thermal behavior of a cold store room filled with bins of dates. The temperature distribution through the row package is determined. The kinetic of the refrigeration process is defined in different locations. The energy consumption of three rows is determined. The room medium needs the more time and more energy for cooling that the other positions and this allows to increase the cost of cooling

References

[1] H. B. Nahor; M. L. Hoang; P. Verboven; M. Boelmans; B. M. Nicolai. (2005): CFD model of the airflow, heat and mass transfer in cool stores. International Journal of Refrigeration 28 (2005), pp. 368-380.
[2] Son. H. Ho; Luis Rosario; Muhammad. M. Rahman, (2010): Numerical simulation of temperature and velocity in a refrigerated warehouse, International Journal of Refrigeration 28 (2010), pp. 1015–1025.
[3] Hong-Minh Hoang; Steven Duret; Denis Flick; Onrawee Laguerre: Preliminary study of airflow and heat transfer in a cold room filled with apple pallets. Comparison between two modelling approaches and experimental results, Applied thermal engineering (2015), pp. 367–381.
[4] Tadhg Brosnan, Da-Wen Sun: Precooling techniques and applications for horticultural products - a review. International Journal of Refrigeration 24 (2001) 15-170.
[5] T. Defraeye, R. Lambrecht, A. A. Tsige, M. A. Delele, U. L. Opara, P. Cronj_e, P. Verboven, B. Nicolai, Forced-convective cooling of citrus fruit: package design, J. Food Eng. 118 (1) (2013) 8-18.
[6] Tressler, D. K., Van Arsdel, W. B., Copley, M. J., Woolrich, W. R., 1968. The Freezing Preservation of Foods. AVI Publishing Company, Westport, CT.
[7] Thijs Defraeye, Rutger Lambrecht, Alemayehu Ambaw Tsige, Mulugeta Admasu Delele,Umezuruike Linus Opara c, Paul Cronjé, Pieter Verboven, Bart Nicolai, Forced-convective cooling of citrus fruit: Package design.
[8] ASHRAE handbook 1998, thermal properties of food.